Multi-Plane Holographic Display with a Uniform 3D Gerchberg-Saxton Algorithm†

Pengcheng Zhou, Yan Li, Chao Ping Chen, Xiao Li, Wei Hu, Na Rong, Yachao Yuan, Shuxin Liu and Yikai Su**

National Engineering Lab for TFT-LCD Materials and Technologies, Department of Electronic Engineering, Shanghai Jiao Tong University, Shanghai, China

Abstract

A modified three-dimensional (3D) Gerchberg-Saxton (GS) algorithm for phase-only holograms in holographic displays is proposed. Numerical and experimental results indicate that compared with the traditional 3D GS algorithm, image-quality difference in the proposed method is reduced by four orders of magnitude, while the average image-quality is increased by 28.7%.

Author Keywords

Holographic display; 3D display; computer holography; image-quality difference; Gerchberg–Saxton algorithm; iterative Fresnel transform algorithm.

1. Introduction

Holographic display is a promising three-dimensional (3D) display technology because it can produce 3D images which can be seen with naked eye as if the images come from actual environments [1-3]. In recent years, holographic displays utilizing computer generated holography (CGH) becomes popular, because it can realize dynamic 3D displays [4]. In CGH, the hologram is calculated by a computer and then written into a display medium, such as a spatial light modulator (SLM), to reproduce the 3D images of a designed object. The pure-phase CGH, known as kinoform [5], has a very high diffraction efficiency due to its non-absorptivity and thus is widely used.

Algorithms of calculating kinoforms include Gerchberg-Saxton (GS) algorithm, direct binary search, simulated annealing (SA), and genetic algorithm (GA), superimposing complex amplitudes from discrete sources with random original phase, and so on. The GS algorithm, originally proposed by Gerchberg and Saxton [6], features many advantages such as less convergence time and clearer reproduction [7] , but it can only reproduce one object plane. Based on the original GS algorithm, 3D GS algorithm [8-11] was developed, which was able to reproduce multiple planes by dividing a 3D object into multiple planes.

However, in the 3D GS algorithm, there is a serious problem in image-quality uniformity along the direction of light propagation. This problem comes from information loss in the iteration loop. And for object planes at different positions, the degree of loss is different, which leads to different reproduced image-qualities consequently. Some modified 3D GS algorithms [12, 13] adopt weighting methods to reduce information loss, so that the image-quality difference can be reduced. But the weighting factors in those algorithms are fixed, and they are not very efficient.

In this paper, a new uniform 3D GS algorithm is proposed to eliminate the image-quality difference. In the new algorithm, the weighting factor is adjusted automatically at different planes in different iteration loops. The adjustment is made based on the feedback from motoring the image-quality difference among all object planes in real-time. With the design, image-quality in each object plane is controlled more subtly and always tends to approach the average image-quality. As a result, the image-quality can be minimized to a large extent. Both numerical simulations and optical experiments are carried out to verify the uniform 3D GS algorithm. The results show that in the new algorithm, the image-quality difference is reduced to 0.209‰ of that in the conventional 3D GS algorithm, and the average quality increases by 28.7%.

2. Vertical image-quality difference in traditional 3D GS algorithm

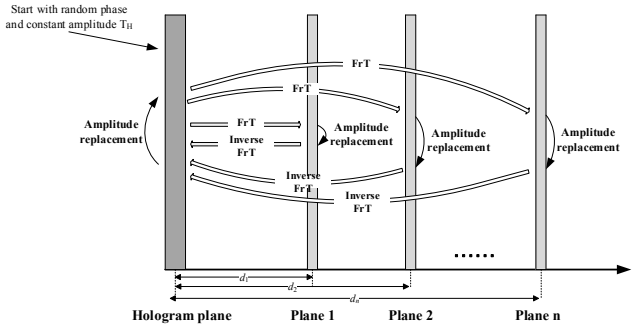

Figure 1. Schematic of the traditional 3D GS algorithm, where the symbol 'FrT' means Fresnel transformation.

The traditional 3D GS algorithm can reproduce multiple planes. As Figure 1 shows, a 3D object is divided into multiple planes and the iteration loop is constructed between object planes and the kinoform plane. Light information goes to and fro between kinoform and each object plane using Fresnel transform and inverse Fresnel transform. The kinoform is further optimized with amplitude replacement in every plane where the phase distribution in is not changed, but the amplitude is replaced with the target amplitude. As a result, the optimized kinoform can approximately reproduce all the target amplitudes in object planes. When the iteration loop comes from kinoform to plane n, the process can be described as below

$$U_n = FrT(U_H) = F_n \cdot \exp(i\varphi_n) \tag{1}$$

$$U_n^{\mathrm{R}} = T_n \cdot \exp(i\varphi_n) \tag{2}$$

$$U_H = IFrT(U_n^R) = F_H \cdot \exp(i\varphi_H) \tag{3}$$

$$U_H^{\mathrm{R}} = T_H \cdot \exp(i\varphi_H) \tag{4}$$

where U and U^R correspond to the complex amplitude before and after amplitude replacement, respectively, FrT and $IFrT$ mean Fresnel transform and inverse Fresnel transform respectively, T is the target amplitude. Eq. (2) and Eq. (4) represent the amplitude replacement in plane n and the kinoform plane, respectively.

The traditional 3D GS algorithm is widely used in 3D holographic displays. However, in the reproduction, image-qualities in different object planes vary and there is large image-quality difference along the direction of light propagation. Therefore,

 ISSN 0097-966X/15/4501-0442-$1.00

some planes are clear but some planes are more blurred or even not recognizable. The main reason is that when enforcing amplitude replacement at one object plane, information of previous planes is lost to some degree. So after a complete iteration loop, information transmitted from object planes to kinoform decays and the degree of decay depends on the positions of object planes in the iteration loop. For example, as shown in Figure 1, the iteration loop is as: kinoform→ plane 1→ plane 2→…→ plane n →kinoform. Plane 1 is the farthest from the final kinoform, so the degree of decay of plane 1 is the highest, and as a result, the image-quality in plane 1 is the worst. On the other hand, plane n is the nearest from the final kinoform, so plane n is the clearest plane. The image-quality difference among those object planes severely degrades the visual effect of the 3D holographic display.

3. Uniform 3D GS algorithm

In the uniform 3D GS algorithm, a weighting amplitude replacement is carried out, where the weighting factors in different planes are self-adjusted based on the feedback from real-time image-quality difference.

(a) Weighting amplitude replacement

The amplitude replacement with the weighting method can be described as follows:

$$U_n^{\mathrm{R}} = (a_n \cdot F_n + (1 - a_n) \cdot T_n) \cdot \exp(i\varphi_n) \tag{5}$$

where a_n is the weighting factor, F_n is the amplitude transmitted from previous plane with Fresnel transform. Compared with amplitude replacement in Eq. (2) and Eq. (4), this amplitude replacement reserves more information from previous object planes and the information loss is reduced. As a result, the image-quality difference among object planes is smaller.

The weighting factor a_{n} can vary in different planes. And we find that in an iteration loop, the weighting factor at one object plane can control the image-quality of that plane. In general, a higher weighting factor leads to a lower image-quality. Based on that, we design a feedback method in which the weighting factor can be automatically adjusted according to the image-quality in every object plane, thus the image-qualities of all planes can be fine-tuned to approach a same value. So the images exhibit uniform qualities.

(b) Self-adjustment of weighting factor according to feedback of image-quality difference

The image-quality can be evaluated by the correlation coefficient (C) between reproduction images and target images, which is defined by:

$$C(t,t_0) = \mathrm{cov}(t,t_0)(\sigma_t \cdot \sigma_{t_0})^{-1} \tag{6}$$

where t is the reproduction amplitude, t_0 represents the amplitude of the target plane, σ is the standard deviation, and cov(t,t_0) is the cross covariance between t and t_0. The C value ranges from 0 to 1. Higher C value means better image-quality. If C equals to 1, the perfect reproduction is obtained.

The self-adjustment process is shown in Figure 2 where $C_1^p, C_2^p, \cdots, C_n^p$ is the image-quality at plane 1, plane 2, $\cdots$,plane n in the pth loop, C_a^p is the average image-quality, $a_1^p, a_2^p, \cdots, a_n^p$ is the weighting factor a at plane 1, plane 2, $\cdots$,plane n in the pth loop. Since the image-quality in one object plane can be controlled by its corresponding weighting factor, image-qualities in all object planes can be adjusted to the same degree by varying the weighting factors. At the end of an iteration loop, image-qualities in all planes and the average image-quality are calculated, based on which the weighting factors of all planes in the next iteration loop are adjusted. If the image-quality in one object plane is higher than the average plane, the weighting factor at the plane in the next iteration loop is increased to reduce the image-quality; if the image-quality is lower, the weighting factor will be reduced. The operation can be enforced by:

$$a_n^{p+1} = a_n^p - (C_n^p - C_a^p)/1000 \tag{7}$$

where the factor 1/1000 is obtained by optimization.

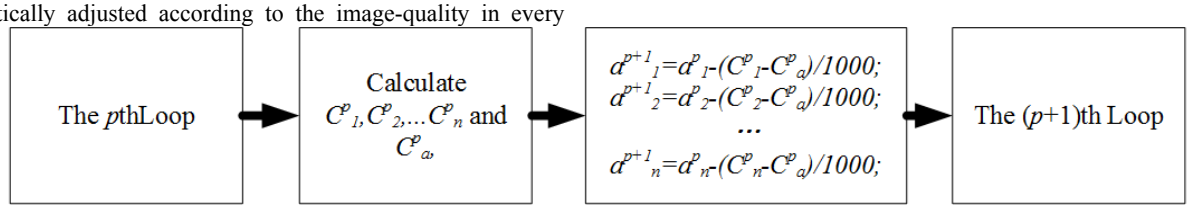

Figure 2. Flowchart of uniform 3D GS algorithm.

4. Experiments and results

(a) Simulation and numerical results

To verify the effectiveness of the uniform 3D GS algorithm in reduction of image-quality difference, numerical simulations using Matlab were performed. In the simulations, the operation wavelength was 488nm. A 3D object was divided into 8 planes. The distance from the kinoform plane to plane 1 was 500 mm, and the distance between two adjacent object planes was 200 mm. The sampling points were 1920 × 1080 in all planes and the sampling interval in the kinoform plane was 8 μm. In our simulations, light propagations were simulated using a convolutional Fresnel method [13], so the sampling interval in each object plane can be calculated as below:

$$\Delta x_n = \frac{\lambda d_n}{1920 * 8\mu m}, \Delta y_n = \frac{\lambda d_n}{1080 * 8\mu m} \tag{8}$$

where Δx_n and Δy_n were the sampling interval in the plane n, d_n is the distance from kinoform to plane n, λ is the operating wavelength. To avoid image-quality difference induced by choosing different target images in different planes, the same target image was used for all object planes, as shown in Figure 3.

Figure 3. Target image in all object planes.

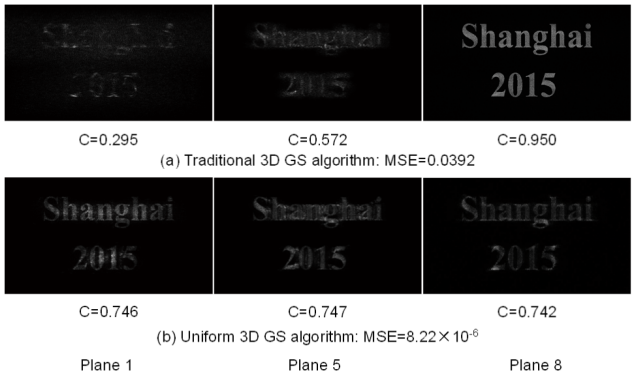

Figure 4. Numerical reproductions in object planes.

Reproductions using the traditional and uniform 3D GS algorithm after 200 iteration loops are shown in Figure 4. For the traditional 3D GS algorithm, obvious image-quality difference can be observed among different object planes. The reproduction in plane 1 is so blurred that one can hardly recognize the original information. From plane 5 to plane 8, the reproduced image qualities gradually increase and the images become more recognizable. More details about the reproduced image-qualities can be found in Table 1 where we used C_a to describe the average image-quality and mean square error (MSE) to describe the image-quality deviation. As indicated in the table, the reproduced image-quality in the traditional 3D GS algorithm varies from 0.295 to 0.950. Plane 6, plane 7 and plane 8 have relatively high image qualities (C>0.6) while plane 1 to plane 5 are hardly recognizable. The image-quality difference greatly affects the visual effect of 3D display.

On the other hand, by using the uniform 3D GS algorithm, the reproduced image-qualities in the eight planes are almost the same. The MSE, indicating the image-quality difference, is 8.22×10^{-6}, which is only 0.209‰ of the value in the traditional method. Besides, all the planes in the uniform 3D GS algorithm are clear. The average image-quality is higher than in traditional 3D GS algorithm, by 28.7%. The reproduction results prove that the uniform 3D GS algorithm can produce high image-quality and good uniformity, which is important for practical 3D holographic displays.

Table 1. Reproduced image-quality in every plane.

	Image-quality								C_a	MSE
	Plane 1	Plane 2	Plane 3	Plane 4	Plane 5	Plane 6	Plane 7	Plane 8		
Traditional 3D GS algorithm	0.295	0.408	0.461	0.509	0.572	0.644	0.785	0.950	0.578	0.0392
Uniform 3D GS algorithm	0.743	0.746	0.747	0.747	0.747	0.739	0.743	0.742	0.744	8.22×10^{-6}

(b) Experimental results

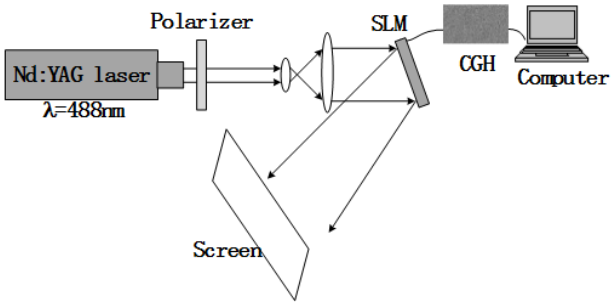

Figure 5. Schematic of the optical setup.

To verify the simulation results, optical experiments were also implemented, as shown in Figure 5. The output kinoform from the two algorithms were written into the spatial light modulator (SLM) illuminated with a collimated laser beam ($\lambda = 488$nm). The SLM is a Holoeye PLUTO VIS SLM, which is pure-phase-modulated, with 1920 × 1080 pixels, 256 grey levels, and a pixel size of 8 μm × 8 μm. The optical reproductions of the two algorithms are presented in Figure 6. The results indicate that there is serious image-quality difference in the reproduction of the traditional 3D GS algorithm. And the reproduced images in plane 1 to plane 5 are so blurred that they can hardly be recognized. As for the uniform 3D GS algorithm, images in all object planes are clear and little image-quality difference can be observed. The results prove the effectiveness in minimizing image-quality difference in 3D display.

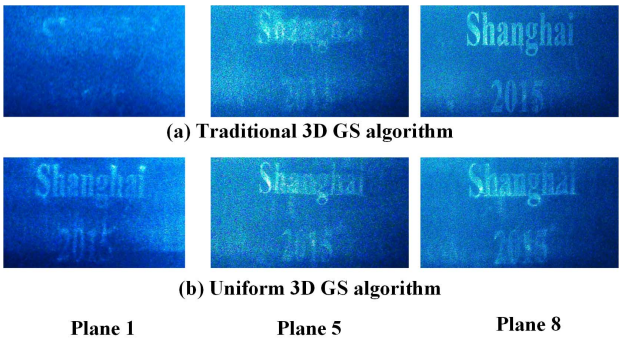

Figure 6. Optical reproductions in object planes.

5. Conclusions

We have proposed a uniform 3D GS algorithm to minimize the image-quality difference along the direction of light propagation. In the proposed algorithm, a novel design of self-adjusting the weighting factor method was employed according to feedback from the image-quality difference Both simulation and experimental results have shown that the uniform 3D GS can improve the image-quality uniformity and average image-quality, which are important for practical 3D holographic displays.

6. Acknowledgements

This work is sponsored by 973 Program (2013CB328804), National Natural Science Foundation of China (61307028, 61405114), and Science & Technology Commission of Shanghai Municipality (13ZR1420000, 14ZR1422300).

7. References

[1] P.-A. Blanche, A. Bablumian, R. Voorakaranam *et al.*, "Holographic three-dimensional telepresence using large-area photorefractive polymer," *Nature,* vol. 468, no. 7320, pp. 80-83, 2010.

[2] M. Huebschman, B. Munjuluri, and H. Garner, "Dynamic holographic 3-D image projection," *Optics Express,* vol. 11, no. 5, pp. 437-445, 2003.

[3] C. P. Chen, Y. Su, and C. G. Jhun, "Recent advances in holographic recording media for dynamic holographic display," Jounal of Optics and Photonic, vol. 1, no. 1, 2014.

[4] K. Wakunami, and M. Yamaguchi, "Calculation for computer generated hologram using ray-sampling plane," *Optics Express,* vol. 19, no. 10, pp. 9086-9101, 2011.

[5] M. Yang, and J. Ding, "Area encoding for design of phase-only computer-generated holograms," *Optics Communications,* vol. 203, no. 1, pp. 51-60, 2002.

[6] R. W. Gerchberg, and W. O. Saxton, "A practical algorithm for the determination of phase from image and diffraction plane pictures," *Optik,* vol. 35, pp. 237-246, 1972.

[7] F. Wyrowski, and O. Bryngdahl, "Iterative Fourier-transform algorithm applied to computer holography," *JOSA A,* vol. 5, no. 7, pp. 1058-1065, 1988.

[8] F. Li, Y. Bi, H. Wang *et al.*, "Weighted 3D GS algorithm for image-quality improvement of multi-plane holographic display," *Chinese Journal of Lasers,* vol. 39, no. 10, pp. 1009001, 2012.

[9] J. Liu, A. Caley, and M. Taghizadeh, "Symmetrical iterative Fourier-transform algorithm using both phase and amplitude freedoms," *Optics Communications,* vol. 267, no. 2, pp. 347-355, 2006.

[10] M. Sypek, A. Kolodziejczyk, and G. MikuĹ, "Three-plane phase-only computer hologram generated with iterative Fresnel algorithm," *Optical Engineering,* vol. 44, no. 12, pp. 125805-125805-7, 2005.

[11] T. Haist, M. Schönleber, and H. Tiziani, "Computer-generated holograms from 3D-objects written on twisted-nematic liquid crystal displays," *Optics Communications,* vol. 140, no. 4, pp. 299-308, 1997.

[12] P. C. Zhou, Y. Bi, M. Y. Sun *et al.*, "Image quality enhancement and computation acceleration of 3D holographic display using a symmetrical 3D GS algorithm," *Applied Optics,* vol. 53, no. 27, pp. G209-G213, Sep, 2014.

[13] C.-f. Ying, H. Pang, C.-j. Fan *et al.*, "New method for the design of a phase-only computer hologram for multiplane reconstruction," *Optical Engineering,* vol. 50, no. 5, pp. 055802, 2011.